RADIOMETRIC PROCESSING SCHEME FOR MULTISPECTRAL ADS40 DATA FOR MAPPING PURPOSES

Ulrich Beisl, System Engineer
Leica Geosystems Geospatial Imaging GmbH
Heinrich Wild Strasse
9435 Heerbrugg, Switzerland
Ulrich.Beisl@gi.leica-geosystems.com

Neil Woodhouse, Software Engineer
Leica Geosystems Geospatial Imaging LLC
10840 Thornmint Road, Suite 100
San Diego, CA 92127, USA
Neil.Woodhouse@gi.leica-geosystems.com

Suqin Lu, System Engineer
Leica Geosystems Geospatial Imaging GmbH
Suqin.Lu@gi.leica-geosystems.com

ABSTRACT

Photogrammetric images are influenced by various effects from outside the camera. One well known effect is the additional path radiance from atmospherically scattered sun light, which gives rise to an increasing blueshift towards the borders of the images. Another effect is the so-called bidirectional reflectance of the ground surface (BRDF). This effect depends on the illumination and the viewing geometry as well as on the wavelength and is caused by a varying amount of subpixel shadows on the ground. Both effects prevent precise intra- and intercomparison of images and impede orthophoto generation and mosaicking. Due to the complex nature of the atmosphere and the unknown conditions at the actual overflight, various approximations have to be made for a fast processing. Two functions for correcting the atmospheric effect have been integrated into the Leica processing chain.

The methods of choice are image based methods: a simple dark pixel subtraction, and a modified dark pixel subtraction with spectral haze prediction. Alternatively, since ADS40 data can be calibrated to at-sensor radiance, physically based methods can be used. It is planned to integrate a Rayleigh correction for fine weather, and a parametrized model for moderate haze, which is using an automatic dark target method for retrieval of the aerosol optical depth. Furthermore, for the bidirectional effect an automated semi-empirical algorithm will be used to obtain either a correction within one image strip or a simultaneous correction of a set of strips to a single illumination and viewing geometry.

INTRODUCTION

The deeper understanding of the radiometric processing is inspired by the higher brightness dynamics and radiometric stability of nowadays digital cameras in contrast to classic film material. Exploiting the higher pixel dynamics of digital cameras will reduce the need for higher resolution as suggested by the General Image Quality Equation GIQE (Leachtenauer et al., 1997): A doubling of the normalized relative edge response RER which is related to the contrast, can compensate for double the ground sampling distance GSD. Furthermore the task of atmospheric correction which was formerly done by filters during image take can now be shifted to digital offline processing which is not time critical and can be tuned.

(Schott, 1997) introduced the idea of an image chain to visualize the different subsequent steps of image generation in remote sensing as the links of a chain. The overall strength of the chain is always determined by the weakest link. However, the usefulness of the chain also depends on the requirements ("weight" vs. "strength")

which are different for photogrammetry and remote sensing. So what is essential for remote sensing is not necessarily important for photogrammetry (cf. **Table 1**).

Although processing speed and data volume are always an issue, in photogrammetry the sheer amount of data to process in a short time requires fast algorithms. Usually, photogrammetry emphasizes the geometric accuracy while remote sensing needs high radiometric quality. But while the knowledge of absolute pixel brightness is not an issue in photogrammetry, there is a need for a color and brightness balanced image. So we still require the correction of atmospheric and bi-directional effects with fast algorithms.

The physics of atmosphere and bi-directional reflection is very complex and the effects show great variability. Both are a field of their own and a lot of information can be derived from analyzing the artifacts. E.g. the blue channel can be used to measure haze and the bi-directional effects contain information about the geometrical properties of the ground at a scale below the geometrical resolution of the camera. But when it comes to produce maps the atmosphere is just a "hostile entity" (Schott, 1997) and bi-directional effects cause annoying borders in mosaicking.

Unfortunately, neither is the theory completely understood, nor is it usually possible to measure the physical parameters which drive the effects at the time when the image is taken. So, left alone, we have to use empirical models which may extract the parameters from the image itself. Two such methods are presented for atmospheric correction and are available in GPro 3.1 for the Leica Photogrammetry Suite: dark pixel subtraction and the modified Chavez method. For describing the bi-directional reflectance a modified Walthall method is suggested.

Table 1. Requirements for radiometric data processing for photogrammetry and remote sensing.

User	Photogrammetry	Remote Sensing
Data Volume	Large	Moderate
Processing speed	High	Moderate
Geometric accuracy	High	Moderate
Radiometric accuracy	Low	High
In-scene radiometric homogeneity	Moderate	High
Atmospheric correction	Empirical	Physical
BRDF correction	Empirical	Empirical or physical

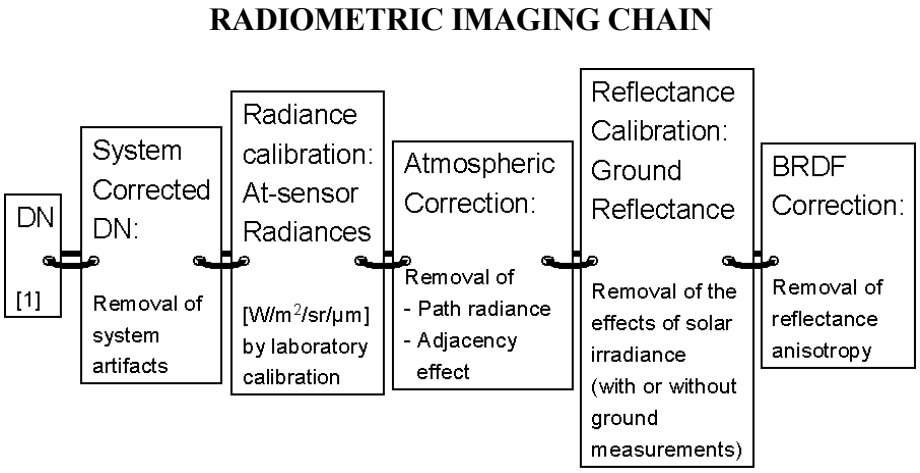

Figure 1. Radiometric imaging chain for the ADS40.

The imaging chain for the radiometric aspect of image processing is shown in **Figure 1**. System artifacts are already corrected in the sensor head so a linear radiometric model can be applied for at-sensor radiance calibration. This allows to relate gray values to a physical quantity called spectral radiance measured in $W/m^2/sr/\mu m$. The radiance calibration is a prerequisite for applying atmospheric corrections based on physical models. It is also useful for empirical atmospheric correction since it creates the same brightness level for all cameras. Reflectance calibration removes the spectral effect of solar irradiance and enables to calculate reflectance, a target property (the

ratio of reflected to incoming light). Finally, once the effects of bi-directional reflection are corrected, a brightness balanced image is created.

RADIANCE CALIBRATION

The simplest radiometric model that can be applied to CCD sensors in good approximation is a linear model. The gray values DN (digital numbers) in level 0 images that result from an incoming band averaged spectral radiance L depend on the calibration factor c_1 and integration time t. An offset c_0 in not necessary, since it is corrected already in the system correction during registration.

$$
\begin{aligned}
L &= \frac{c_1\, DN}{t} \\
L &\quad \left[W/\left(m^2 sr\, \mu m\right)\right] \\
c_1 &\quad \left[Ws/\left(m^2 sr\, \mu m\, DN\right)\right] \\
DN &\quad [1] \\
t &\quad [s]
\end{aligned}
\tag{1}
$$

The specific calibration factor c_1 is a sensor constant and is provided in the "RADIOMETRIC_GAIN" value in the geometric calibration file (*.cam) of the ADS40 sensor head. The "RADIOMETRIC_GAIN" values are calculated from laboratory measurements of a uniform white target (cf. **Figure 2**). The c_1 values are measured during camera production and are available from Leica on request. Though the camera is radiometrically stable a recalibration can ensure radiometric accuracy.

In order to keep the image data in a 16 bit unsigned integer data range (0-65535) the radiances are scaled during level 1 rectification in Leica's GPro software by a factor of 50 to give calibrated digital numbers CDN. From GPro 3.x on, once the "RADIOMETRIC_GAIN" values are provided in the *.cam files, the CDN for each pixel are calculated from the original DN by

$$CDN = DN * 50\, c_1 / t \tag{2}$$

So the processed image is calibrated to spectral at-sensor radiances although still unsigned integer values can be used. Please note that the calibration is omitted if a tonal transfer curve (TTC) is applied during level 1 rectification. The band averaged spectral radiance L of the band is easily calculated by

$$L = CDN/50 \tag{3}$$

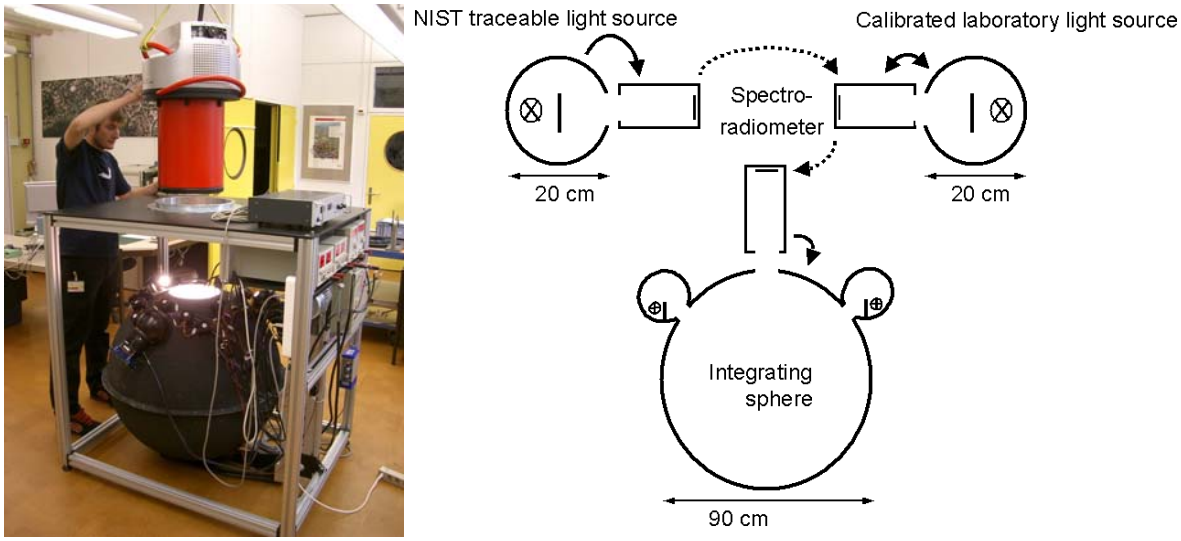

Figure 2. Radiometric calibration facility (left) and calibration procedure for the integrating sphere (right).

The result of the calibration is the following (cf. **Figure 3**):

- The brightness of the Pan band is shifted such that it is comparable to the RGB bands.
- The brightness of the RGB bands is shifted such that any ADS40 camera will produce the same brightness level in each color if there is the same illumination.

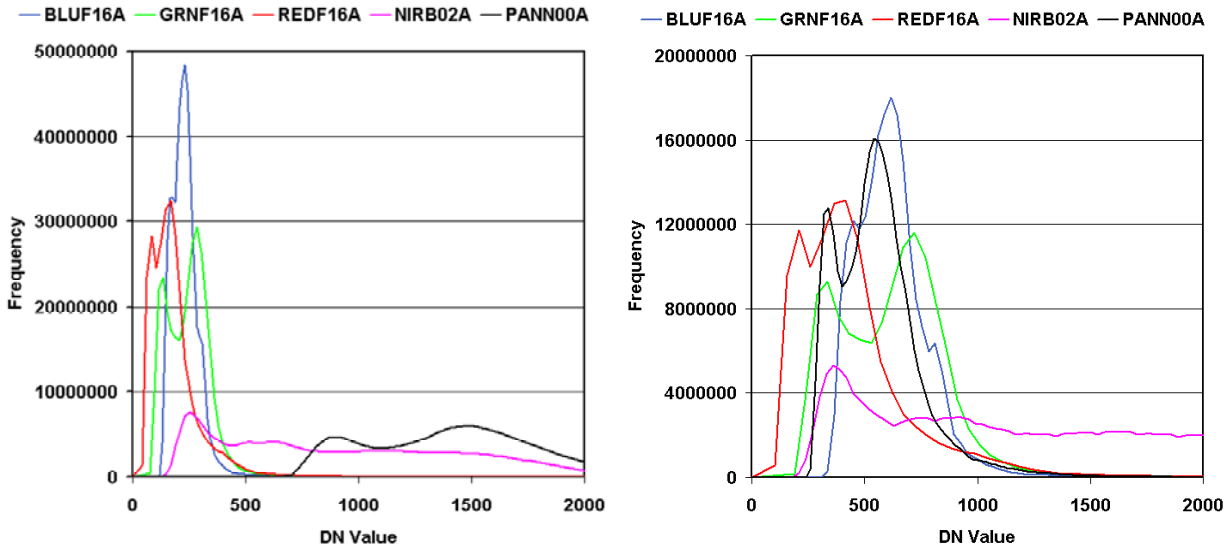

Figure 3. Histogram of the color and pan lines of an image before (left) and after (right) radiance calibration.

ATMOSPHERIC CORRECTION

Path Radiance

On its way from sun to ground and from ground to sensor, light is scattered by gaseous and aerosol particles. The additional light reaching the sensor which does not originate from the ground is called path radiance. This is the largest contribution to atmospheric effects. Scattering increases with atmospheric path length and is therefore view angle dependent. This gives rise to an increasing blue shift towards the borders of the images. In a line scanner geometry this causes linear effects in contrast to circular effects in frame imagery.

Methods that correct for the path radiance can be divided into image based empirical and physical model based methods. Physical models, e.g. MODTRAN (Berk et al., 1998), require radiometrically calibrated data and some input of atmospheric data. The latter is often missing for most image data apart from a visual impression of "haziness". So although physical methods are more accurate, a good time is spent on guessing the right values for the atmospheric parameters.

Therefore if only a color balanced image is needed often image based empirical methods are preferred. They do not necessarily need radiometric calibration. An issue for all models is to incorporate the regional changes in atmosphere and the change in atmospheric path length due to changing ground elevation.

Dark Pixel Subtraction

The dark pixel subtraction (Chavez, 1975) assumes that the path radiance in the specified area is an additive constant to the pixel brightness which has to be subtracted. Therefore the subtraction value is equal to the image brightness of a completely dark ground target. So an image histogram will show an offset where the pixel frequency has non-zero values (cf. **Figure 4**.). The view angle dependence is taken into account by calculating column statistics and correcting column-wise. The detection of the dark pixel is rather conservative in order to prevent over-correction, taking the lowest 0.1 % of the total pixels as dark pixel threshold.

A major drawback of Chavez' method is that the histogram offsets are determined independently for each band. As can bee seen from **Figure 4** the offset decreases from blue to green, red and Near Infrared because the haze effect for the longer wavelength bands decreases. So depending on the actual statistics the chance of subtracting too much in the longer wavelength bands is rather high, especially if dark pixels are rare.

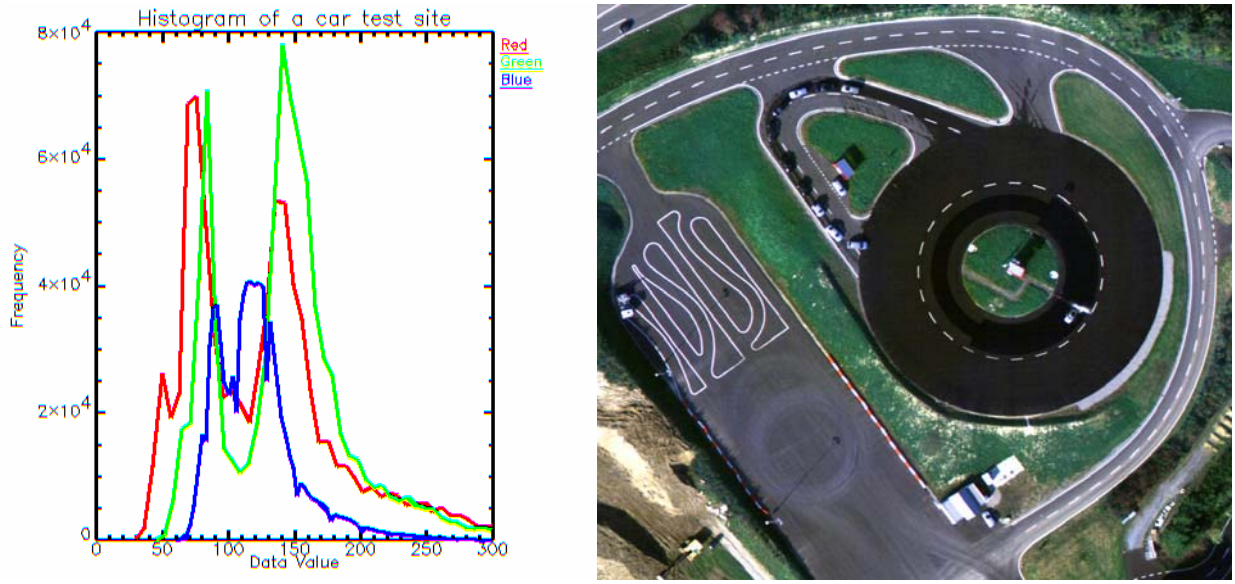

Figure 4. Histogram of an uncalibrated image of a car test site (Oct 13th, 2003). The histograms for each color start at an RGB-offset of 35, 50, and 70 pixels, respectively, which is removed in dark pixel subtraction.

Modified Chavez Method

So Pat Chavez has improved the dark pixel subtraction by setting up a relationship between the different offsets (Chavez, 1988). He assumes a $\lambda^{-\kappa}$ rule for the decreasing haze effect which is inspired by the λ^{-4} rule of Rayleigh scattering (cf. **Figure 5**). The value of κ depends on the overall haze in the image. A decreasing κ value refers to increasing haze, i.e. aerosol scattering.

The idea now is to determine the dark pixel offset of the blue channel which is particularly affected by haze, and to predict the values for the other bands. This prevents an overcorrection for the red and NIR bands.

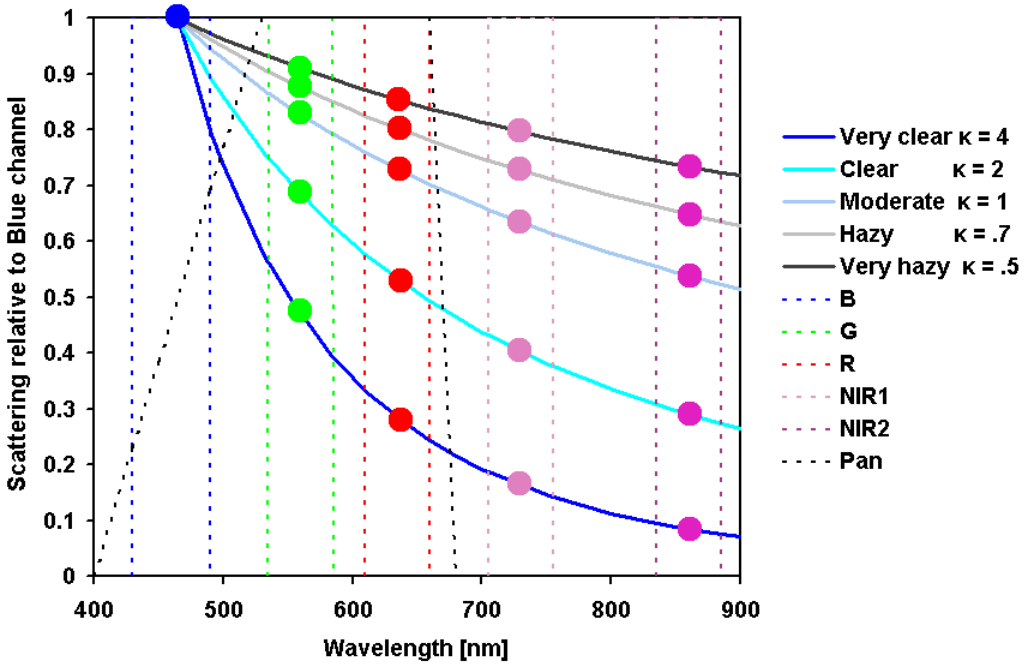

Figure 5. Wavelength dependence of the atmospheric scattering for different haze models $\lambda^{-\kappa}$.

The model value κ is determined by the following selection rule. Height dependent boundary values L_{pb} for the different atmospheric models are calculated and the actual blue channel offset value L is determining the κ value (cf. **Table 2**).

Table 2. Selection rule for model parameter κ

Atmosphere	Visibility [km]	Rule	K
Very clear	> 80	$L < L_{pb}(80, h)$	4
Clear	30 – 80	$L_{pb}(80, h) < L < L_{pb}(30, h)$	2
Moderate	12 – 30	$L_{pb}(30, h) < L < L_{pb}(12, h)$	1
Hazy	5 – 12	$L_{pb}(12, h) < L < L_{pb}(5, h)$	.7
Very hazy	< 5	$L > L_{pb}(5, h)$	.5

Figure 6 shows the height dependence of the path radiance for different atmospheric models, calculated with the MODTRAN software. Considering only flight heights over 1 km then a linear regression is sufficient. This regression is used to calculate the height dependent boundary values L_{pb}. The automatic setting will use this selection rule. In case of a special atmospheric situation the setting can be adjusted manually.

The height dependence shows already a possible error source: The calculation is done with an average flying height. In case of a rugged terrain this height will change and with it the atmospheric path length. In a future version a DEM will have to be used to calculate areas of equal height with their respective haze model.

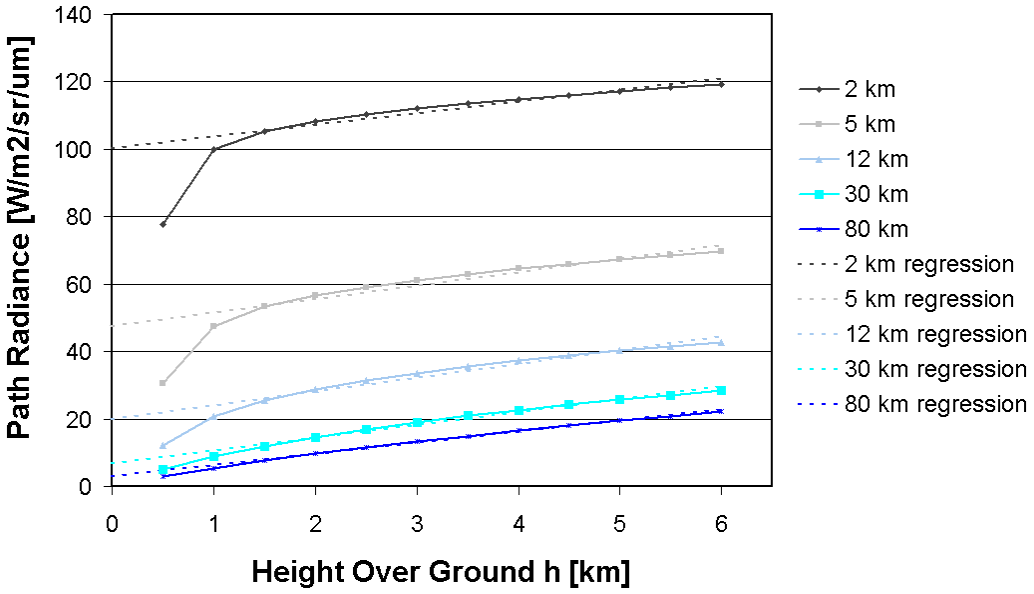

Figure 6. Height dependence of the path radiance for different visibilities calculated with MODTRAN for a midlatitude summer atmosphere with rural aerosols.

REFLECTANCE CALIBRATION

Assuming that the absorption from ground to sensor is small, we can calculate the ground radiance by subtracting the path radiance from the at-sensor radiance. The ground radiance is still influenced by the spectrum and intensity of the solar irradiation, so it will depend on the solar elevation and atmospheric conditions. In order to calculate a surface property it is necessary to divide the ground radiance by the solar irradiance. Again this involves using a physical model and having atmospheric parameters.

This step will be taken after releasing a Rayleigh correction for fine weather, and a parametrized model for moderate haze, which is using an automatic dark target method for retrieval of the aerosol optical depth.

BRDF CORRECTION

Bi-directional effects which are described by the bi-directional reflectance distribution function (BRDF), originate from the reflection properties of the ground and have an impact on image quality of the same order of magnitude as atmospheric effects. The effect depends on the illumination and viewing geometry and can be seen as a brightening towards the borders of the image similar to the atmospheric effects which impedes mosaicking. But while the atmosphere creates a blue hue, the BRDF is in general wavelength independent and changes only in the photosynthetic active wavelength range (Beisl, 2001).

At high solar elevation (noon) in regions with low geographical latitude a prominent effect occurs, the so-called hot spot and is well known from aerial images. It is located opposite the specular reflection point (cf. **Figure 7**). Due to the central perspective the effect has got a circular shape and appears whenever the solar zenith angle is smaller than the cameras‘ half field of view. Line scanner images have a linear symmetry and therefore show a linear hot spot. It appears only when a pixel viewing direction is aligned with the Sun illumination direction. Since the ADS40 features only discrete lines, hot spot features can be avoided by careful flight planning. If there is the possibility of hot spots (solar elevation larger than 70°) the simplest method, which also minimizes other BRDF effects, is to align the flight line with the solar azimuth. Another method is to avoid flight times where solar elevation is larger than 70° (noon).

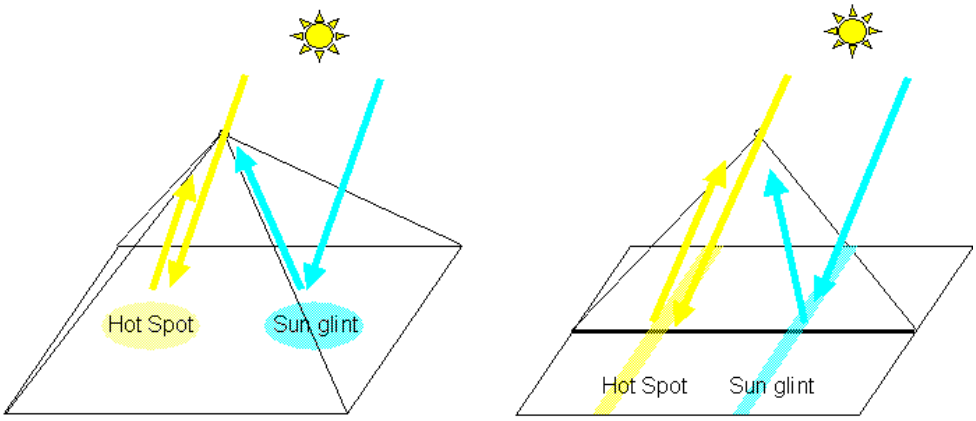

Figure 7. Hot spot and sun glint in frame cameras (left) and line scanners (right).

BRDF effects are supposed to be predominantly shadow-driven. Therefore a linear mixing approach can be taken. Then the pixel brightness R is in the first order proportional to the ratio x of the illuminated pixel area to the total pixel area. This holds true if this ratio is small or if there is cast shadow, i.e. small haze. In this case the correction should be inverse proportional to the pixel brightness.

$$R(\theta) = x(\theta)\rho_{hot\,spot} + (1 - x(\theta))\rho_{shadow} \approx x(\theta)\rho_{hot\,spot} \quad (4)$$

$$\rho_c(\theta) = \rho(\theta) * (R(\theta_c)/R(\theta)) \quad (5)$$

where

$\rho(\theta)$, $\rho_c(\theta)$	observed and corrected reflectance
$R(\theta)$	modeled reflectance
θ, θ_c	view and correction zenith angle
x	ratio of illuminated to total area within one pixel

Modified Walthall Method

In 1985, Charles Walthall proposed a simple empirical equation to describe the in-scene variation of reflectance (Walthall, 1985), having a view zenith and relative azimuth dependence. This was improved by Nilson and Kuusk in 1989 by introducing a solar zenith dependence (Nilson and Kuusk, 1989). In order to include hot spot effects an additional term coming from analytical models is included (Beisl and Woodhouse, 2004).

The resulting linear semi-empirical model (**Equation 6**) is easy to invert, applies to any surface and includes a hot spot term. Due to its view and solar angle dependence it can be used to correct a complete image block simultaneously (Beisl, 2002). The model is applied to each color band separately. A correction can be calculated either for all pixels or class specific.

$$R(\theta_i, \theta_r, \varphi) = a\theta_i^2\theta_r^2 + b(\theta_i^2 + \theta_r^2) + c\theta_i\theta_r\cos\varphi + dD + e \quad (6)$$

where

R	modeled reflectance
θ_i	incident illumination zenith angle
θ_r	reflection view zenith angle
φ	relative azimuth angle
a,b,c,d,e	free parameters

$D = \sqrt{\tan^2\theta_i + \tan^2\theta_r - 2\tan\theta_i\tan\theta_r\cos\varphi}$ hot spot term

DATA AND RESULTS

As an example for atmospheric correction, a rural area is shown, taken in October 13th 2003 at 3 p.m. local time from 2500 m above ground. The terrain varies from 500 m (S) to 700 m (N) above sea level. The calibrated image shows a lot of haze which is increasing towards the borders. The simple dark pixel correction works well, since all histograms are populated in the lower values. The automatic haze setting for the modified Chavez method had to be changed from very clear to clear. An example for the correction of bi-directional effects can be found in (Beisl and Woodhouse, 2004).

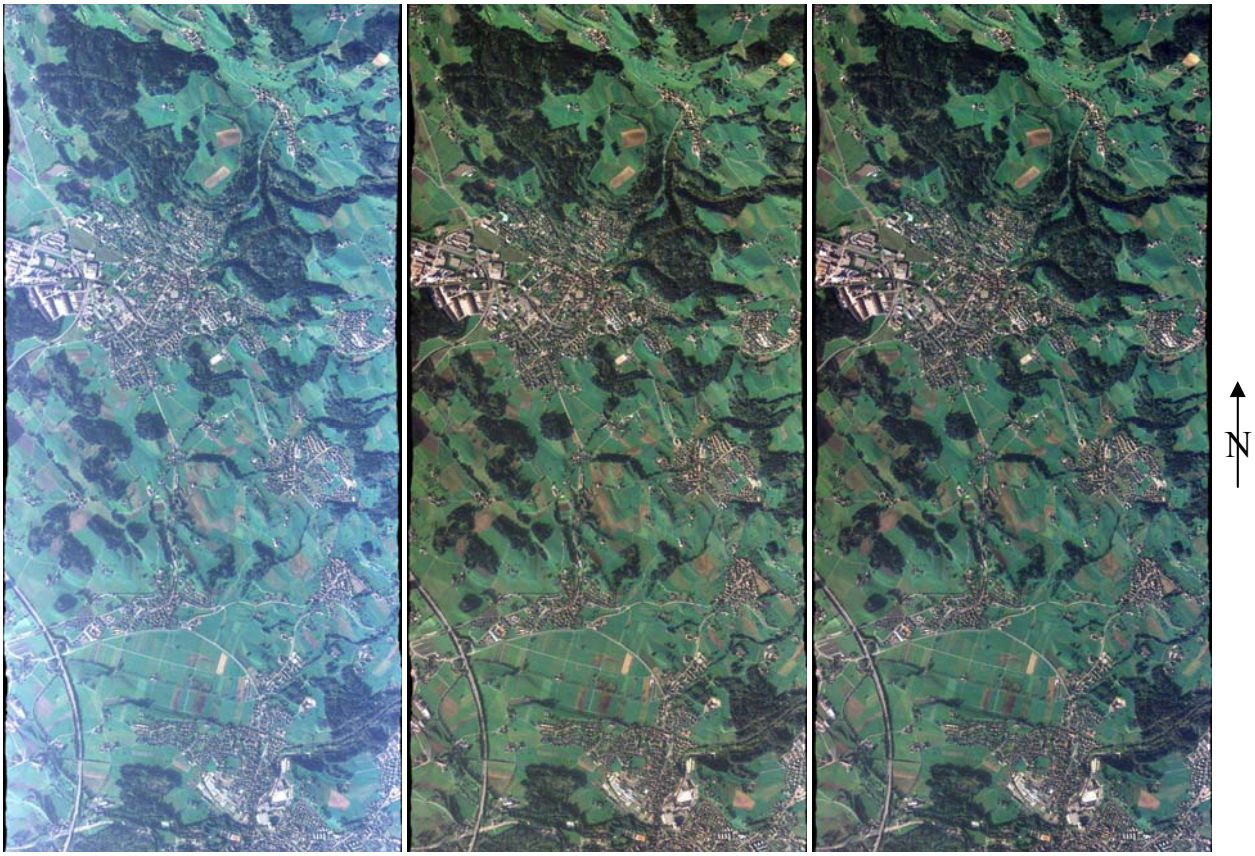

Figure 8. A calibrated image (left) is compared with a simple dark pixel correction (middle) and a modified Chavez method (right) with settings "rural" and "clear". The stretching for all colors in all images is linear from 0-1200 DN.

CONCLUSIONS

In this paper we have shown a strategy for correction of atmospheric and BRDF effects in ADS40 images. The requirements for mapping imagery differ from those in remote sensing applications. The huge data amounts require fast and robust algorithms which produce seamless image mosaics. So empirical methods are the first choice unless the data quality requires higher accuracy.

For the case of the atmospheric correction this results in using either a simple or an improved dark pixel method. A BRDF correction can be performed using an improved Walthall model. It was shown with ADS40 RGB image data that the blue hue from atmospheric effects could be removed and - together with a radiometric calibration - a color balanced image could be produced that does not need any special stretching. This is a step towards an automatic generation of huge seamless maps.

REFERENCES

Beisl, U. (2001). *Correction of bidirectional effects in imaging spectrometer data*. Remote Sensing Laboratories, University of Zurich, Remote Sensing Series, 37, 184 pp.

Beisl, U. (2002). Simultaneous correction of bidirectional effects in line scanner images of rural areas. *Proc. 9th International Symposium in Remote sensing (SPIE)*, Agia Pelagia, Crete.

Beisl, U., and N. Woodhouse (2004). Correction of atmospheric and bidirectional effects in multispectral ADS40 images for mapping purposes. *Proc. XXth Congress of the ISPRS,* Istanbul, Turkey, 12-23 July. 5 p.

Berk, A., L.S. Bernstein, G.P. Anderson, P.K. Acharya, D.C. Robertson, J.H. Chetwynd, and S.M. Adler-Golden (1998). MODTRAN cloud and multiple scattering upgrades with application to AVIRIS. *Remote Sens. Environ., 65,* 367-375.

Chavez, P. S. Jr. (1975). Atmospheric, solar, and MTF corrections for ERTS digital imagery. *Proc. Am. Soc. Photogrammetry*, Fall Technical Meeting, Phoenix, AZ, p. 69.

Chavez, P. S. Jr. (1988). An improved dark-object subtraction technique for atmospheric scattering correction of multispectral data. *Remote Sens. Environ., 24*: 459-479.

Leachtenauer, J.C., W. Malila, J. Irvine, L. Colburn, and N. Salvaggio (1997). General image-quality equation: GIQE. *Appl. Opt., 36*(32), 8322-8328.

Nilson, T., and A. Kuusk (1989). A reflectance model for the homogeneous plant canopy and its inversion. *Remote Sens. Environ., 27*: 157-167.

Schott, J. R. (1997). *Remote Sensing: The image chain approach.* Oxford University Press, New York.

Walthall, C. L., J.M. Norman, J.M. Welles, G. Campbell, and B.L. Blad (1985). Simple equation to approximate the bidirectional reflectance from vegetative canopies and bare soil surfaces. *Appl. Opt., 24*(3), 383-387.